"Physics of Auroral Phenomena", Proc. XLVI Annual Seminar, Apatity, pp. 19-22, 2023

DOI: 10.51981/2588-0039.2023.46.004

SUBSTORMS CAUSED BY LARGE-AMPLITUDE SOLAR WIND DYNAMIC PRESSURE PULSES: CASE STUDY ON 3 NOVEMBER 2021

L.I. Gromova[1], N.G. Kleimenova[2], I.V. Despirak[3], S.V. Gromov[1], L.M. Malysheva[2], A.A. Lubchich[3]

[1]*Pushkov Institute of Terrestrial Magnetism, Ionosphere, and Radio Wave Propagation, Moscow, Troitsk, Russia;* e-mail: *gromova@izmiran.ru*
[2]*Schmidt Institute Physics of the Earth RAS, Moscow, Russia*
[3]*Polar Geophysical Institute, Apatity, Russia*

Abstract. We studied the geomagnetic effects of abrupt and large-amplitude changes in the solar wind dynamic pressure (*Psw*) on 3 November 2021. when there were observed three large-amplitude *Psw* pulses (up to 20 nPa) under the strong (up to −18 nT) southward IMF *Bz* and significantly varying IMF *By* (from +20 to −15 nT). Basing on IMAGE magnetometer data, we found three substorms associated with these *Psw* impulses. These substorms followed one after another with a short interval and each subsequent substorm began developing during the unfinished recovery phase of the previous one under disturbed space weather conditions. Under strong negative IMF *Bz* there was significant input of energy into the magnetosphere that indicated by the increasing *PC*-index values. It was shown that the spatial-temporal features of the substorm subsequence development was complicated, differed from a typical isolated "normal" substorm and changed from one substorm to another. According to the AMPERE 66 ionospheric satellite data, the global distribution of the ionospheric and field-aligned currents (FAC) was established during the considered substorms. We found that during all these substorms, there were strong FACs and corresponding ionospheric electrojets in the morning sector indicating an enhanced magnetospheric convection which formed the DP2 current system. In addition, in the night sector, the DP1 current system was observed, the clearest in the second event.

Introduction

Geomagnetic effects of abrupt and large-amplitude changes in the solar wind dynamic pressure (*Psw*) have been studied for a long time and resulted in many works [e.g., *Akasofy*, 1964; *Tsurutani and Meng*, 1972; *Kokubun et al.*, 1977; *Akasofu and Chao*, 1980; *McPherron*, 1991; *Tsurutani and Zhou*, 2003; *Liou and Newell*, 2010; *Sinha et al.*, 2023 and many others]. It was concluded that a substorm initiation was accelerated by the shock-induced compression of the magnetosphere [*Kokubun et al.*, 1977] and the substorms followed shock impacts represent the result of increases in the rate of direct energy transfer from the solar wind. [*Akasofu and Chao*, 1980]. There were established main properties of the electrojet development [*Wiens and Rostoker*, 1975], and its dependence on the sign and magnitude of IMF *By* [*Liou and Newell*, 2010].

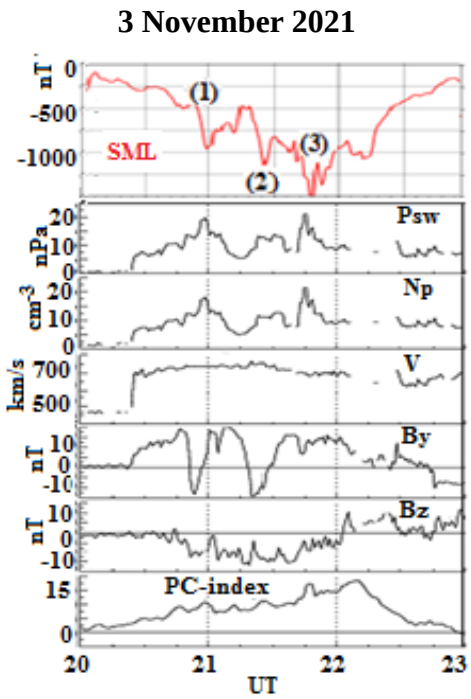

Figure 1. The IMF and the solar wind parameters, and geomagnetic activity indices.

As a rule, only isolated substorms have been analyzed, however, most often, substorms follow one after another with a short interval.

The aim of this paper is to study the spatial-temporal feature of the of substorm subsequence observed on 3 November 2021.

There were three large-amplitude pulses of the solar wind dynamic pressure *Psw* (up to 20 nPa) under high values of the solar wind speed (~800 km/s), the IMF *Bz* (up to −18 nT) and significantly varying IMF *By* (from +20 to −15 nT) that caused the subsequence of three substorms with *SML*-index increasing from one substorm to another of ~ −900, −1100, −1500 nT (see Fig.1). The values of the *PC*-index also increased in time in this substorm subsequence.

Our study was based on magnetic data of the IMAGE and INTERMAGNET magnetometer networks and the AMPERE satellite global maps of the ionospheric and the field-aligned current (FAC). Data from sites https://space.fmi.fi/image/, https://intermagnet.org/, https://supermag.jhual.edu/,

https://omniweb.gsfc.nasa.gov/, https://pcindex.org/, https://ampere.jhuapl.edu/.

Ground based observations

During the time interval of 20-23 UT, the IMAGE meridian chain was in the mid-night sector (23-02 MLT). The IMAGE magnetograms (*X* and *Z* components) from the high latitude stations and map of the ionospheric equivalent current distribution (Fig. 2) demonstrate that the substorm (1) was observed like a "normal" substorm at 64-68° MLAT, and the second one shifted equatorward up to 60-64° MLAT. The third substorm unexpectedly shifted poleward with the huge (up to 1000 nT) abrupt intensification at the latitudes higher BJN station (71° MLAT). The third substorm was observed in the very large latitude range, from ~60° up to ~77° MLAT (Fig. 2b, c). Thus, we may refer it to the so called "expanded" substorm [*Despirak et al.*, 2014, 2019] since it was observed under a high solar wind speed (Fig. 1). This substorm demonstrated a very complicated latitudinal structure. However, it should be note that there is the sea between BJN and NOR stations, and there are no the ground-based data.

As one can see in Fig. 2d, all three considered events were accompanied by mid-latitude positive magnetic bays in the *X* component at PAG and KIV stations. The *Y* component was positive in the substorms (1) and (2) and it was negative in the substorm (3). It was interpreted as the location of the center of the substorm current wedge (SCW) eastward from the IMAGE meridian in the events (1) and (2) and it was westward in the event (3).

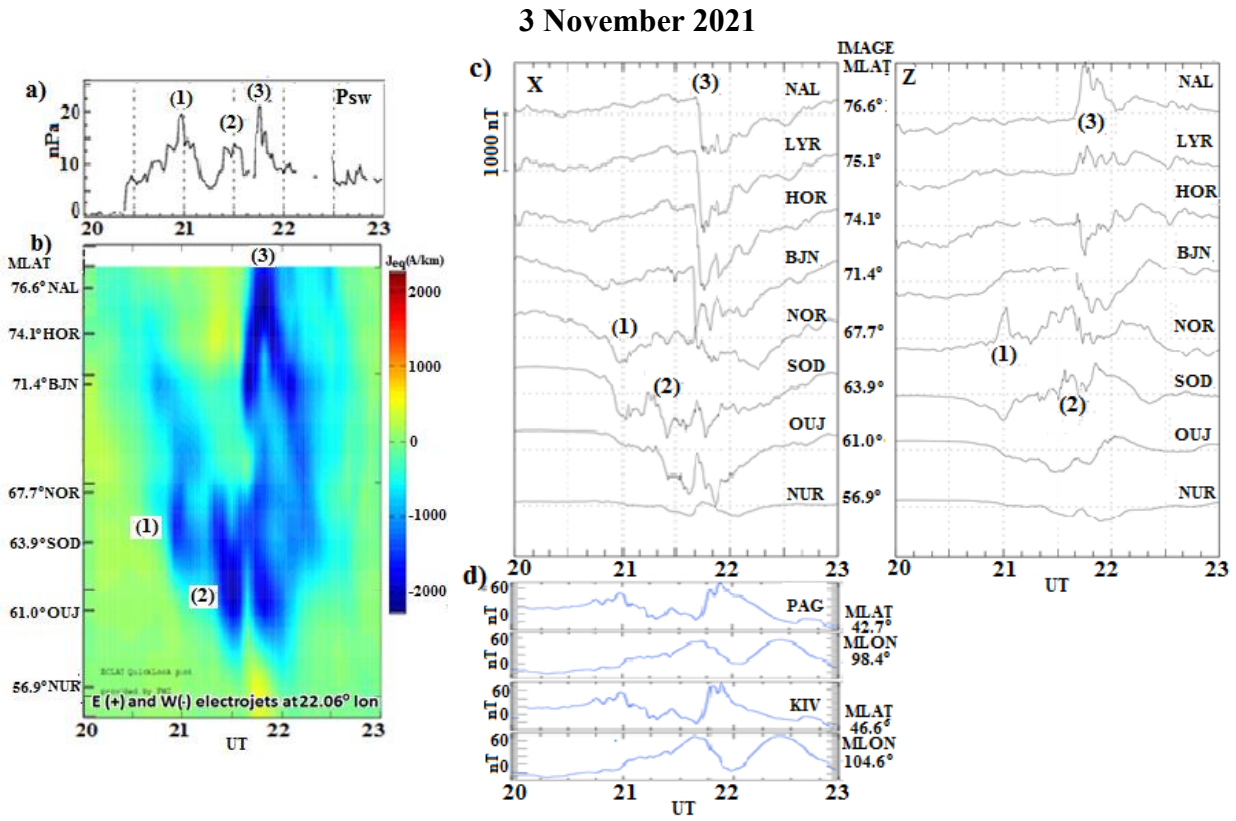

Figure 2. (a) Three large-amplitude pulses of *Psw*; (b) ionospheric equivalent currents calculated from ground-based IMAGE magnetometers; (c) IMAGE high-latitude station *X* and *Z* components; (d) INTERMAGNET magnetograms of mid-latitude stations located close to the same meridian as IMAGE stations.

Global distribution of the ionospheric and field-aligned currents according to the AMPERE maps

The global maps of the ionospheric and field-aligned currents distributions are derived by the AMPERE project based on the simultaneous magnetic measurements of the 66 low-altitude satellites globally distributed at the altitude of ~780 km as 10-min averages with the 2 min cadence. Figs 3-5 show the AMPERE maps in the time intervals correspondent to the maxima of the considered substorms (see the *SML*-index in Fig.1).

Fig. 3 demonstrates that during the *SML*-maximum of the substorm (1), the strongest intensification of the westward electrojet and FACs was observed in the morning sector (04-08 MLT) at ~65° MLAT. The Scandinavian IMAGE magnetometer chain measured only its high-latitude westward part. Note, that during this substorm, the strong electrojets and FACs were observed in the daytime sector as well.

As it is shown in Fig. 4, during the *SML*-maximum of the substorm (2), the strongest intensification of the westward electrojet and FACs, was located in the morning sector (04-06 MLT) like in substorm (1). However, the new substorm occurred near midnight (22-03 MLT) at the latitudes of ~60-70° MLAT. The IMAGE magnetometers chain found

themselves near the center of this electrojet, due to that, the intensity of the substorm (2) was greater than of the substorm (1). The eastward electrojet shifted to lower latitudes up to 62° MLAT and enhanced in the longitude up to 21 MLT. In the dayside, the FACs and ionospheric electrojet remained strong and complicated.

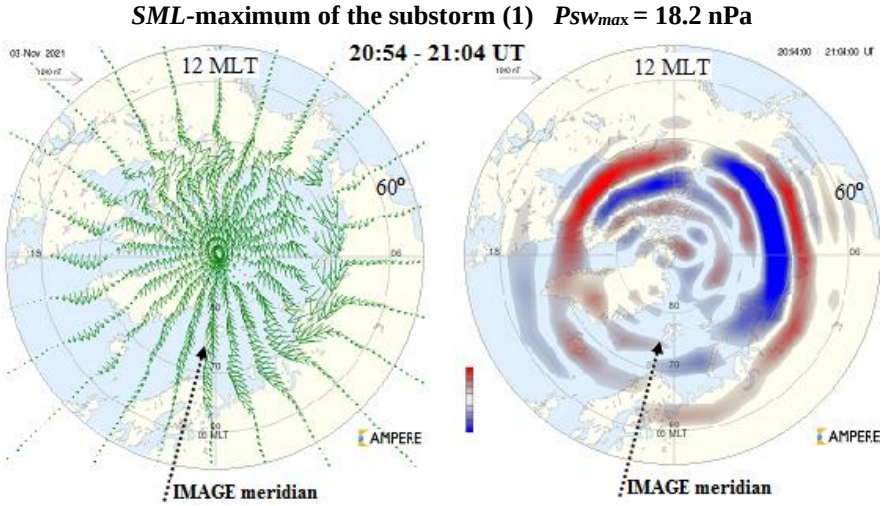

Figure 3. Substorm (1): AMPERE global maps of the ionospheric (left) and the field-aligned currents (right) distributions. Downwards FACs is in blue, upwards ones is in red. Dotted arrow shows IMAGE meridian direction.

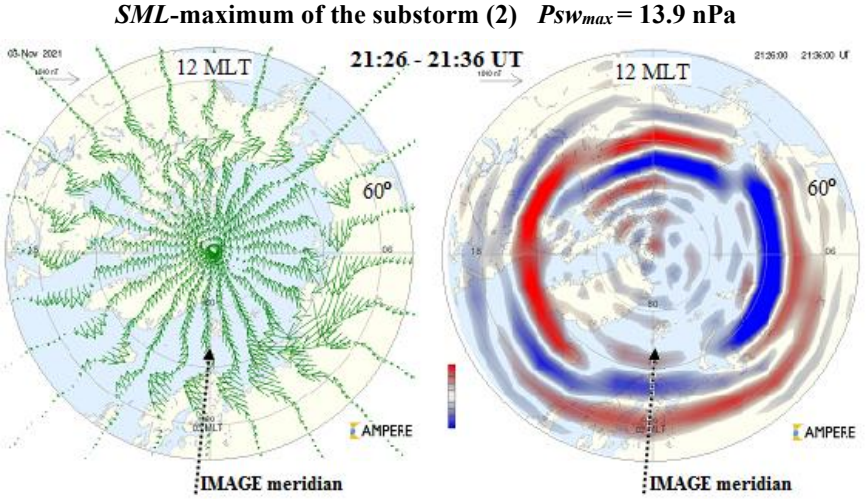

Figure 4. The same as in Fig. 3 but for the substorm (2).

The ionospheric current and FACs distributions during substorm (3) are shown in Fig. 5. This substorm could be referred to an "expanded" type of substorm since according to the AMPERE satellite data, the westward ionospheric current was recorded in the late evening sector from ~60° MLAT to 76° MLAT, i.e., in more larger latitude region than in the early morning sector. It is should be noted that the "expanded" substorm occurred after the change the sign of IMF *By* from negative to positive.

The considered substorms followed one after another with a short interval and each subsequent substorm began developing during the unfinished recovery phase of the previous one under disturbed conditions.

Besides, the substorms (1) and (2) observed under strong negative IMF *By* (about −15 nT). But before pulse (3) of the solar wind dynamic pressure, IMF *By* sharply changed to the strong positive values (up to +15 nT). We could suppose that such the IMF *By* behaver caused the complicated FACs distribution in the event (3).

We found that during all considered substorms, there were strong FACs and corresponding ionospheric to electrojets in the morning sector indicating an enhanced magnetospheric convection (as well as the values of *PC*-index) formed the DP2 current system. The addition DP1 system is most clearly seen during the substorm (2).

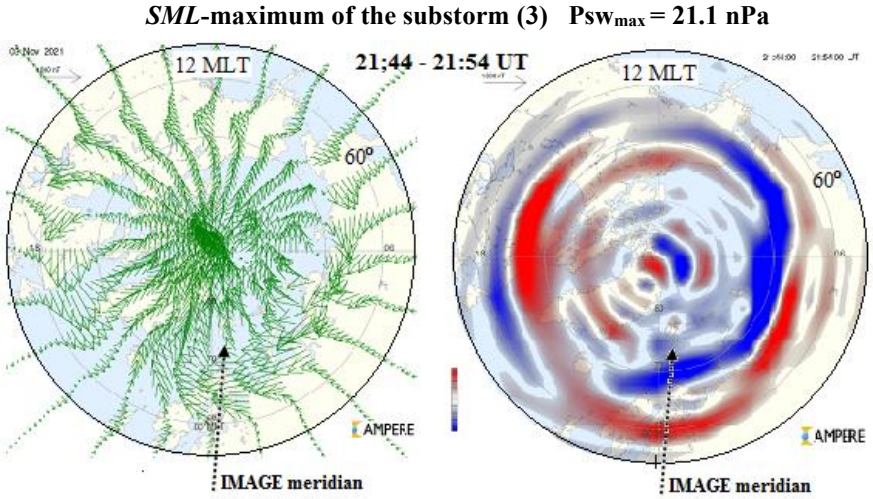

Figure 5. The same as Fig. 3 but for the magnetic-bay (3).

Conclusion

The analysis of the magnetic data of the event of 3 November 2021 showed that some spatial-temporal features of the substorm subsequence caused by large-amplitude solar wind dynamic pressure pulses were complicated, differed from a typical isolated "normal" substorm and changed from one substorm to another. Each substorm developed during the unfinished recovery phase of the previous substorm under disturbed space weather conditions.

The main geoeffective parameters of the solar wind and IMF, such as the solar wind speed and IMF *Bz* values, did not change during this substorm subsequence. Despite this, the features of the considered substorms were different that indicates an important role of other parameters of the solar wind and, probably, previous magnetic conditions.

References

Akasofu S.-I. The development of auroral substorm // Planet. Space Sci., V. 12, pp. 273–282, 1964.

Akasofu S.-I., Chao J.K. Interplanetary shock waves and magnetospheric substorms // Planet. Space Sci., V. 28, pp. 381–385, 1980. https://doi.org/10.1016/0032-0633(80)90042-2

Despirak I.V., Lyubchich A.A., and Kleimenova N.G. Polar and high latitude substorms and solar wind conditions // Geomagnetism and Aeronomy, V. 54, No. 5, pp. 575–582, 2014. https://doi.org/10.1134/S0016793214050041

Despirak I.V., Lyubchich A.A., and Kleimenova N.G. Solar Wind Streams of Different Types and High-Latitude Substorms // Geomagnetism and Aeronomy, V. 59, No. 1, pp. 1–6, 2019. https://doi.org/10.1134/S0016793219010055

Kokubun S., McPherron R.L., Russell C.T. Triggering of substorms by solar wind discontinuities // J. Geophys. Res., V. 82, No. 1, pp. 74–86, 1977. https://doi.org/10.1029/JA082i001p00074

Liou K., Newell P.T. On the azimuthal location of auroral breakup: Hemispheric asymmetry // Geophys. Res. Lett., V. 37, No. 23, pp. 1–5, 2010. https://doi.org/10.1029/2010GL045537

McPherron R.L. Physical processes producing magnetospheric substorms and magnetic storms // Geomagnetism, V. 4, pp. 593–739, 1991.

Sinha S., Vichare G., Sinha A.K. A comparative analysis of the role of interplanetary magnetic field (IMF) and sudden impulse (SI) in triggering a substorm // Advances in Space Research, V. 71, pp. 97-114, 2023. https://doi.org/10.1016/j.asr.2022.08.037

Tsurutani B.T., Meng C.-I. Interplanetary magnetic-field variations and substorm activity // J. Geophys. Res., V. 77. No. 16, pp. 2964–2970, 1972. https://doi.org/10.1029/JA077i016p02964

Tsurutani B.T., Zhou X.-Y. Interplanetary shock triggering of substorms: WIND and Polar // Adv. Space Res., V.31, No. 4, pp. 1063–1067, 2003. https://doi.org/10.1016/S0273-1177(02)00796-2

Wiens R.G., Rostoker G. Characteristics of the development of the westward electrojet during the expansive phase of magnetospheric substorms // J. Geophys. Res., V. 80, pp. 2109–2128, 1975.